

Defect structures in sine-Gordon like models

D. Bazeia, L. Losano and R. Menezes

*Departamento de Física, Universidade Federal da Paraíba,
Caixa Postal 5008, 58051-970 João Pessoa, Paraíba, Brazil*

(Dated: October 1, 2018)

We investigate several models described by real scalar fields, searching for topological defects. Some models are described by a single field, and support one or two topological sectors, and others are two-field models, which support several topological sectors. Almost all the defect structures that we find are stable and finite energy solutions of first-order differential equations that solve the corresponding equations of motion. In particular, for the double sine-Gordon model we show how to find small and large BPS solutions as deformations of the BPS solution of the ϕ^4 model. And also, for most of the two field models we find the corresponding integrating factors, which lead to the complete set of BPS solutions, nicely unveiling how they bifurcate among the several topological sectors.

PACS numbers: 03.50.-z, 05.45.Yv, 03.75.Fi, 05.30.Jp

I. INTRODUCTION

This work deals with kinks and domain walls in sine-Gordon like models in $(1, 1)$ spacetime dimensions. They are extended classical solutions of topological profile, supposed to play important role in several different contexts as for instance in condensed matter [1, 2] and in high energy physics [3, 4].

Models described by real scalar fields in $(1, 1)$ space-time dimensions are among the simplest systems that support topological solutions. Usually, the topological solutions are classical static solutions of the equations of motion, with topological behavior related to the asymptotic form of the field configurations. The topological profile can be made quantitative, with the inclusion of the topological current, $j_T^\mu = (1/2)\varepsilon^{\mu\nu}\partial_\nu\phi$. It gives the topological charge $Q_T = (1/2)(\phi(x \rightarrow \infty) - \phi(x \rightarrow -\infty))$, which is not zero when the asymptotic value of the field differs in both the positive and negative directions. To ensure that the classical solutions have finite energy, one requires that the asymptotic behavior of the solutions is identified with minima of the potential that defines the system under consideration, so in general the potential has to include at least two distinct minima in order for the system to support topological solutions.

We can investigate real scalar fields in $(3, 1)$ space-time dimensions, and now the topological solutions are named domain walls. These domain walls are bidimensional structures that carry surface tension, which is identified with the energy of the classical solutions that spring in $(1, 1)$ space-time dimensions. The domain wall structures are supposed to play a role in applications to several different contexts, ranging from the low energy scale of condensed matter [1, 2, 5, 6] up to the high energy scale required in the physics of elementary particles, fields and cosmology [3, 4, 7].

There are at least three classes of models that support kinks or domain walls, and we further explore such models in the next Sec. II. In the first class of models one deals with a single real scalar field, and the topological solutions are structureless. Examples of this are the sine-Gordon and ϕ^4 models [3]. In the second class of models one also deals with a single real scalar field, but now the systems comprise at least two distinct domain walls. An example of this is the double sine-Gordon model, which has been investigated for instance in Refs. [8, 9, 10, 11, 12, 13]. In the third class of models we deal with systems defined by two real scalar fields, where one finds domain walls that admit internal structure [14, 15, 16, 17, 18, 19, 20], and junctions of domain walls, which appear in models of two fields when the potential contains non-collinear minima, as recently investigated for instance in Refs. [21, 22, 23, 24, 25, 26, 27, 28, 29, 30, 31, 32, 33]. We study new possibilities in Sec. III, and there we investigate periodic systems, which present several topological sectors, which may bifurcate into richer structures. For most of them, we find the integrating factors, which lead us to all the BPS solutions the models engender.

There are other motivations to investigate domain walls in models of field theory, one of them being related to the fact that the low energy world volume dynamics of branes in string and M theory may be described by standard models in field theory [34, 35, 36]. Besides, one knows that field theory models of scalar fields may also be used to investigate properties of quasi-linear polymeric chains, as for instance in the applications of Refs. [37, 38, 39, 40], to describe solitary waves in ferroelectric crystals, the presence of twistons in polyethylene, and solitons in Langmuir films.

Domain walls have been observed in several different scenarios in condensed matter, for instance in ferroelectric crystals [6], in one-dimensional nonlinear lattices [41], and more recently in higher spatial dimensions – see [42] and references therein. The potentials that appear in the models of field theory that we investigate in the present work are also of interest to map systems described by the Ginzburg-Landau equation, since they may be used to explore

the presence of fronts and interfaces that directly contribute to pattern formation in reaction-diffusion and in other spatially extended, periodically forced systems [2, 5, 43, 44, 45, 46].

For completeness, in Sec. IV we investigate other topological sectors of the periodic two field models, where the domain wall solutions are of the non-BPS type. And finally, we end the paper in Sec. V, where we include our comments and conclusions.

II. SINGLE FIELD MODELS

In this work we are interested in field theory models that describe real scalar fields and support topological solutions of the Bogomol'nyi-Prasad-Sommerfield (BPS) type [47, 48]. In the case of a single real scalar field ϕ , we consider the Lagrange density

$$\mathcal{L} = \frac{1}{2}\partial_\mu\phi\partial^\mu\phi - V(\phi) \quad (1)$$

Here $V(\phi)$ is the potential, which identifies the particular model under consideration. We write the potential in the form

$$V(\phi) = \frac{1}{2}W_\phi^2 \quad (2)$$

where $W = W(\phi)$ is a smooth function of the field ϕ , and $W_\phi = dW/d\phi$. In a supersymmetric theory W is the superpotential, and this is the way we name W in this work.

The equation of motion for $\phi = \phi(x, t)$ has the general form

$$\frac{\partial^2\phi}{\partial t^2} - \frac{\partial^2\phi}{\partial x^2} + \frac{dV}{d\phi} = 0 \quad (3)$$

and for static solutions we get

$$\frac{d^2\phi}{dx^2} = W_\phi W_{\phi\phi} \quad (4)$$

It was recently shown in Refs. [49, 50] that this equation of motion is equivalent to the first order equations

$$\frac{d\phi}{dx} = \pm W_\phi \quad (5)$$

if one is searching for solutions that obey the boundary conditions $\lim_{x \rightarrow -\infty} \phi(x) = \bar{\phi}_i$ and $\lim_{x \rightarrow -\infty} (d\phi/dx) = 0$, where $\bar{\phi}_i$ is one among the several vacua $\{\bar{\phi}_1, \bar{\phi}_2, \dots\}$ of the system. In this case the topological solutions are BPS (or anti-BPS) states. Their energies get minimized to the value $t^{ij} = |\Delta W_{ij}|$, where $\Delta W_{ij} = W_i - W_j$, with W_i standing for $W(\bar{\phi}_i)$. The BPS solutions are defined by two vacuum states belonging to the set of minima that identify the several topological sectors of the model.

In a recent work [51] one has introduced a deformation prescription, in which one defines a deformation function $f = f(\phi)$, which allows introducing new models presenting defect solutions. The deformation prescription goes as follows: if we change the potential $V(\phi)$ to $\tilde{V}(\tilde{\phi})$, given by

$$\tilde{V}(\tilde{\phi}) = V(\phi \rightarrow f)/(df/d\tilde{\phi})^2 \quad (6)$$

where $f = f(\tilde{\phi})$ is a well-defined, invertible function, then the defect solution of the new model can be obtained as

$$\tilde{\phi}(x) = f^{-1}(\phi(x)) \quad (7)$$

where $\phi(x)$ represents the defect solution of the former model. More recently, in another work [52] one has enlarged the scope of the procedure, using other deformations.

A. Single field. One kink solutions

We now turn attention to kinks and domain walls. Perhaps the most known example of this is given by the ϕ^4 model, defined by the potential $V(\phi) = \frac{1}{2}\lambda^2 (v^2 - \phi^2)^2$, where we are using natural units. In this model the domain wall can be represented by the solution $\phi_s(x) = \pm v \tanh(\lambda vx)$. The above potential can be written with the superpotential $W(\phi) = \lambda(v^2\phi - \phi^3/3)$, and the domain wall is of the BPS type. The wall tension corresponding to the BPS kink is $t_s = 4/3|\lambda v^3|$.

Another example of system described by one field can be generated from the above ϕ^4 model, using the deformation method [51, 52] with the deformation function $f(\phi) = v \sin(v\phi)$. In this case we obtain the sine-Gordon model defined by the potential

$$V = \frac{1}{2}\lambda^2 \cos^2(v\phi) \quad (8)$$

with the kink and antikink solutions

$$\phi(x) = \pm \frac{1}{v} \arcsin[\tanh(\lambda vx)] + k\pi \quad (9)$$

This potential can be written with the superpotential $W(\phi) = (\lambda/v) \sin(v\phi)$, and the kink is of the BPS type. There is an infinite set of minima given by $\phi = k\pi/v$, where k is positive or negative integer. The wall tension corresponding to the BPS wall is $t_s = 2|\lambda/v|$.

B. Single field. Two kink solutions

We can build another class of models, in which the domain walls engender other features. We refer to models described by a single field, but the systems may now support two or more distinct topological solutions. An interesting example of this is the double sine-Gordon model defined by the potential,

$$V = \frac{\lambda^2}{2\alpha^2 v^2} [\cos^2(v\phi) - \alpha^2 \sin^2(v\phi)]^2 \quad (10)$$

which can be generated from the ϕ^4 model above, employing the deformation function $f_1(\phi) = \alpha \tan(v\phi)$ or $f_2(\phi) = \frac{1}{\alpha} \tan(v\phi - \frac{\pi}{2})$. It is interesting to see that if one uses the deformation prescription with the f_1 -deformation, we get the solutions

$$\phi_1(x) = \pm \frac{1}{v} \arctan\left(\frac{1}{\alpha} \tanh(\lambda x)\right) + \frac{n\pi}{v} \quad (11)$$

However, if one uses the f_2 -deformation there are new solutions, given by

$$\phi_2(x) = \mp \frac{1}{v} \arctan(\alpha \tanh(\lambda x)) + \frac{(2n+1)\pi}{2v} \quad (12)$$

These solutions represent large kinks and small kinks, which appear in the double sine-Gordon model. The novelty here is that we are finding the large and small kink solutions, using the deformation procedure of Refs. [51, 52]. In Fig. 1, we depict the behavior of the potential in Eq.(10), in terms of the parameter α . There we see the double sine-Gordon models, and we also show the topological sectors corresponding to the solutions $\phi_1(x)$ and $\phi_2(x)$.

The potential (10) does not give double sine-Gordon behavior as λ and v vary, for $\alpha = 1$. Thus, since we shall concentrate the investigation on the double sine-Gordon model, which profile depends only on α , we prefer to change the potential to the form

$$V_r(\phi) = \frac{1}{r+1} [4r \cos(\phi) + \cos(2\phi)] \quad (13)$$

where r is a parameter, real and positive. This potential is periodic, with period 2π , and for simplicity in the following we consider the interval $-2\pi < \phi < 2\pi$. The value $r = 1$ distinguishes two regions, the region $r \in (0, 1)$ where the potential contains four minima, and the region $r \geq 1$, where the potential contains two minima. For $r \in (0, 1)$ the system supports two distinct wall configurations, the large wall and the small wall, which distinguish the two different barrier the model comprises in this case. The limits $r \rightarrow 0$ and $r \rightarrow \infty$ lead us back to the sine-Gordon model, with period π and 2π , respectively. The double sine-Gordon model has been considered in several distinct applications, as

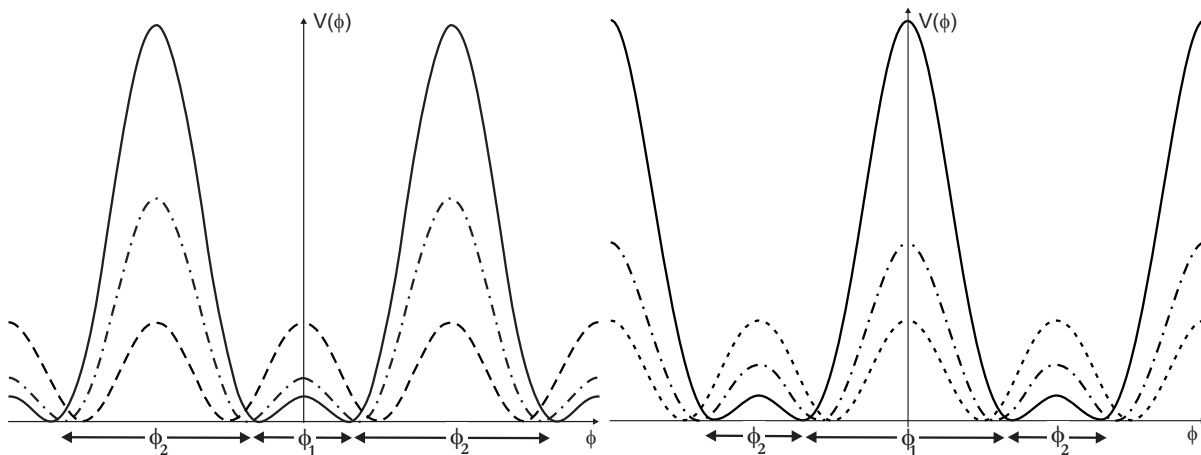


FIG. 1: The double sine-Gordon model. The left figure shows the case $\lambda = v = 1$, for $\alpha = 1$ (dashed line), $\alpha = 1.5$ (dash-dotted line), and $\alpha = 2$ (solid line). The right figure shows the case $\lambda = v = 1$ for $\alpha = 1$ (dotted line), $\alpha = 0.75$ (dash-dotted line), and $\alpha = 0.50$ (solid line).

for instance in Ref. [8, 9, 10], where one investigates magnetic solitons in superfluid ^3He , kink propagation in a model for poling in polyvinylidene fluoride, and properties related to the two different kinks that appear in such polymeric chain. More recently, it has also been used to model magnetic solitons in uniaxial antiferromagnetic systems [53].

To expose new features of the double sine-Gordon model we rewrite Eq. (13) in the form

$$V_r(\phi) = \frac{2}{1+r} [\cos(\phi) + r]^2 \quad (14)$$

where we have omitted an unimportant r -dependent constant. This potential is a particular case of the potential (10), with $\alpha = \sqrt{(1-r)/(1+r)}$, $v = 1/2$, and $\lambda = \sqrt{1-r}$. Thus, it is a deformation of the ϕ^4 model, and can be described by the superpotential

$$W(\phi) = \frac{2}{\sqrt{1+r}} [\sin(\phi) + r\phi] \quad (15)$$

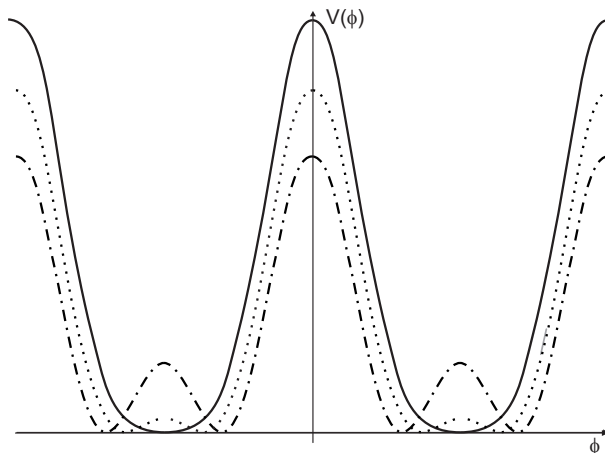


FIG. 2: The double sine-Gordon potential, depicted for $r = 1/3$ (dash-dotted line), $r = 2/3$ (dotted line), and $r = 1$ (solid line), to illustrate how the behavior of the model changes with r . Our notation is such that both $V(\phi)$ and ϕ are dimensionless, as we explain in the work.

For r in the interval $r \in (0, 1)$ the minima of the potential are the singular points of the superpotential, $dW/d\phi = 0$. They are periodic, and for $-2\pi < \phi < 2\pi$ there are four minima, at the points $\bar{\phi} = \pm\pi \pm \alpha(r)$, where $\alpha(r) = \arccos(r)$.

For $r \geq 1$ the minima are at $\bar{\phi} = \pm\pi$, in the interval $-2\pi < \phi < 2\pi$. A closer inspection shows that for $0 < r < 1$ the local maxima at $\pm\pi$ and the minima $\pm\pi \pm \alpha(r)$ degenerate to the minima $\pm\pi$ for $r = 1$, and remain there for $r > 1$. Thus, the parameter r induces a transition in the behavior of the double sine-Gordon model.

The value $r = 1$ is the critical value, since it is the point where the system changes behavior: for $r \in (0, 1)$ this model supports minima that do *not* appear for $r \geq 1$. We illustrate the double sine-Gordon model in Fig. [2], where we depict the potential (14) for $r = 1/3, 2/3$ and for $r = 1$. Thus, it is very interesting to see that this model maps the presence of magnetic solitons in uniaxial systems [53]: in fact, the model is able to model both the antiferromagnetic, canted and weak ferromagnetic phases. In particular, in the canted phase there are two different domain walls connecting minima between two different barriers, as we show below.

To get a better view of the the double sine-Gordon model, we examine the order parameter $\bar{\phi}(r)$, which is given by $\pm\pi \pm \alpha(r)$ for $0 < r \leq 1$, so it goes continuously to $\pm\pi$ for $r \geq 1$. Also, the (squared) mass of the field can be obtained via the relation

$$V_r''(\bar{\phi}) = W_{\bar{\phi}}^2 + W_{\bar{\phi}} W_{\bar{\phi}\bar{\phi}} \quad (16)$$

where $\bar{\phi}$ is the corresponding minimum of the potential. For $0 < r \leq 1$ we get $m^2(r) = 4 - 4r$, and for $r \geq 1$ we have $m^2(r) = 4(r - 1)/(r + 1)$. We see that $m(r)$ vanishes in the limit $r \rightarrow 1$. These results indicate that r mimics a second order phase transition, a transition where the system goes from the case of two distinct phases to another one, engendering a single phase, as one illustrates in Fig. 3.

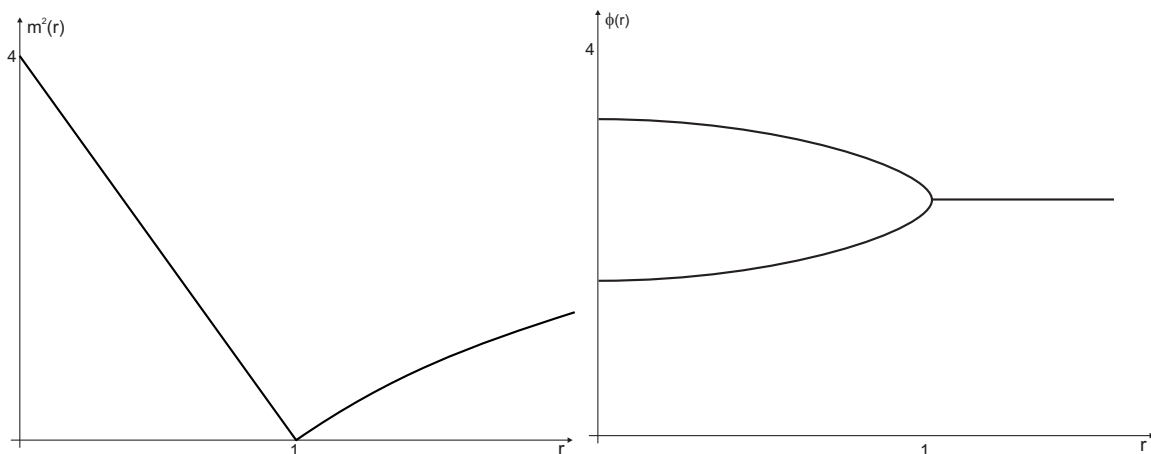


FIG. 3: Plots of $m^2(r)$ (left) and $\bar{\phi}(r)$ (right) for the double sine-Gordon potential, which illustrate how the behavior of the model changes with r . The quantities $\bar{\phi}$, $m(r)$, and r that appear in these figures are all dimensionless.

Let us first consider the case $0 < r \leq 1$. The energies of the BPS solutions are given as follows. For solutions connecting the minima $-\pi + \alpha(r)$ and $\pi - \alpha(r)$ the defect is large since it joins minima separated by a higher and wider barrier. We have

$$t_{dsG}^l = 4\sqrt{1-r} + 4r \frac{\pi - \alpha(r)}{\sqrt{1+r}} \quad (17)$$

In the case of the minima $\pi - \alpha(r)$ and $\pi + \alpha(r)$ the defect is small and we get

$$t_{dsG}^s = 4\sqrt{1-r} - 4r \frac{\alpha(r)}{\sqrt{1+r}} \quad (18)$$

We notice that $t_{dsG}^l = t_{dsG}^s + 4\pi r/\sqrt{1+r}$, and the limit $r \rightarrow 1$ sends $t_{dsG}^l \rightarrow 2\sqrt{2}\pi$ and $t_{dsG}^s \rightarrow 0$, as expected. For the BPS states, from Eqs. (11) and (12) we can write the solutions explicitly. For instance, for solutions that connect the minima $-\pi + \alpha(r)$ and $\pi - \alpha(r)$ we get large kink solutions, which are of the form

$$\phi_l(x) = \pm 2 \arctan \left[\sqrt{\frac{1+r}{1-r}} \tanh(\sqrt{1-r} x) \right] \quad (19)$$

For solutions that connect the minima $\pi \pm \alpha(r)$ and the minima $-\pi \pm \alpha(r)$ we get small kink solutions. They are given by

$$\phi_s(x) = \pm\pi - 2 \arctan \left[\sqrt{\frac{1-r}{1+r}} \tanh(\sqrt{1-r}x) \right] \quad (20)$$

The case $r > 1$ is different. The minima are now at $\pm\pi$, and the model is similar to the standard sine-Gordon model. In this case we modify the potential of Eq. (14) to

$$V(\phi) = \frac{2}{r+1}(\cos^2(\phi) + 2r \cos(\phi) + 2r - 1) \quad (21)$$

to make $V(\pm\pi) = 0$. Thus, we can write this potential in terms of another superpotential, such that

$$\widetilde{W}_\phi = \frac{2}{\sqrt{r+1}} \sqrt{\cos^2(\phi) + 2r \cos(\phi) + 2r - 1} \quad (22)$$

The presence of the square root complicates the calculation, and we have been unable to find explicit analytical solutions in this case.

The potential in Eq. (14) in the limit $r \rightarrow 0$ goes to $V_0(\phi) = 1 + \cos(2\phi)$ which leads us back to the sine-Gordon model. Thus, we can suppose r small and use $V_r(\phi)$ to explore the double sine-Gordon model as a model controlled by a small parameter, in the vicinity of the sine-Gordon model. This feature is of direct interest to investigations that follow the lines of Ref. [54], which explores the vicinity of the BPS bound, and also in the case concerning the presence of internal modes of solitary waves, which seems to appear when one slightly modifies integrable models – see for instance Ref. [55].

III. TWO FIELD MODELS

We now turn attention to another class of models, which is described by two real scalar fields. In this case the domain walls may engender internal structure; see, e.g., Refs. [14, 15, 16]. In the present work we are interested in models of the sine-Gordon type, but now described by two real scalar fields.

In the case of two real scalar fields ϕ and χ , the potential is written in terms of the superpotential, in a way such that

$$V(\phi, \chi) = \frac{1}{2} W_\phi^2 + \frac{1}{2} W_\chi^2 \quad (23)$$

The equations of motion for static fields are

$$\frac{d^2\phi}{dx^2} = W_\phi W_{\phi\phi} + W_\chi W_{\chi\phi} \quad (24)$$

$$\frac{d^2\chi}{dx^2} = W_\phi W_{\phi\chi} + W_\chi W_{\chi\chi} \quad (25)$$

which are solved by the first order equations

$$\frac{d\phi}{dx} = \pm W_\phi \quad \frac{d\chi}{dx} = \pm W_\chi \quad (26)$$

Solutions to these first order equations constitute the BPS states of the model. They solve the equations of motion, and have energy minimized to $t^{ij} = |\Delta W^{ij}|$ as in the case of a single field; here, however, $\Delta W^{ij} = W(\phi_i, \chi_i) - W(\phi_j, \chi_j)$, since now we need the pair (ϕ_i, χ_i) to represent each one of the vacuum states in the system of two fields. An important issue is that in the plane (ϕ, χ) one may have minima that are noncolinear, and this opens the possibility for junctions of defects. Moreover, in the case of two real scalar fields we can find a family of first-order equations that are equivalent to the pair of second-order equations of motion, but this requires that $W_{\phi\phi} + W_{\chi\chi} = 0$, in the case of harmonic superpotentials [49, 50].

Models described by two real scalar fields are more intricate, and require more involved investigations. For instance, to solve the two first-order equations one can search for the integrating factor [56]. However, the integrating factor is in general hard to find, and so we can use the trial orbit method, as suggested in [57] in detail.

The models that we investigate are of interest both to ferromagnetic [53] and ferroelectric [58] systems. They are defined by the following general potential

$$V(\phi, \chi) = \frac{1}{2}\eta^2 \{ [r + \cos(\phi) \cos(p\chi)]^2 + p^2 \sin^2(\phi) \sin^2(p\chi) \} \quad (27)$$

where the parameter p is real and positive, with $p \neq 1$ [the case $p = 1$ leads to single field models with a $\pi/2$ rotation in the (ϕ, χ) plane]. We will consider three distinct models, with $r = 0$, $0 < r < 1$, and $r \geq 1$. The case $r = 0$ and $r \geq 1$ describe two coupled sine-Gordon models, and the case $0 < r < 1$ describe two coupled double sine-Gordon models. These models are new, and some of their features will be examined below.

In general, all the three models can be described by the following superpotential

$$W(\phi, \chi) = \eta [r\phi + \sin(\phi) \cos(p\chi)] \quad (28)$$

and this will help simplifying the investigation, since the BPS solutions satisfy first order differential equations, which are simpler to solve compared to the equations of motion.

In this section we search for BPS solutions in the models introduced in this paper. We investigate the first order equations corresponding to each one of the three models separately. For model 1 and model 2 we obtain the integrating factors, which allow solving the first order equations completely, finding all the family of orbits which connect the minima of the potential with energy minimized to BPS states.

A. Model 1

The first model is given by the potential (27) with $r = 0$. In terms of the superpotential (28) the first order equations are

$$\frac{d\phi}{dx} = \eta \cos(\phi) \cos(p\chi) \quad (29)$$

$$\frac{d\chi}{dx} = -\eta p \sin(\phi) \sin(p\chi) \quad (30)$$

There are minima at the points $v_{n,m} = ((2n+1)\pi/2, m\pi/p)$ and $w_{n,m} = (n\pi, (2m+1)\pi/2p)$. In Fig. 4 we display these minima in the plane $(\phi, p\chi)$.

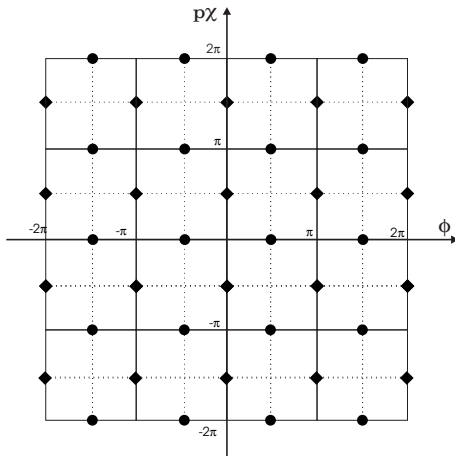


FIG. 4: The minima of model 1 potential. The minima v are represented by balls, and w by losangles.

To obtain the most general solution to the first-order Eqs. (29) and (30), we integrate the ordinary differential equation

$$\frac{d\phi}{d\chi} = -\frac{1}{p} \cot(\phi) \cot(p\chi) \quad (31)$$

which admits the integrating factor $\sin^{-\sigma}(p\chi)$, with $\sigma = 1 + 1/p^2$, and this determines all the orbits connecting the minima via the family of curves

$$\cos(\phi) = C \frac{1}{p} \sin^{\sigma-1}(p\chi) \quad (32)$$

where C is a real integration constant. In fig. 5, the behavior of a particular orbit with C , in the family (32) is displayed, where the critical value is $C = p$.

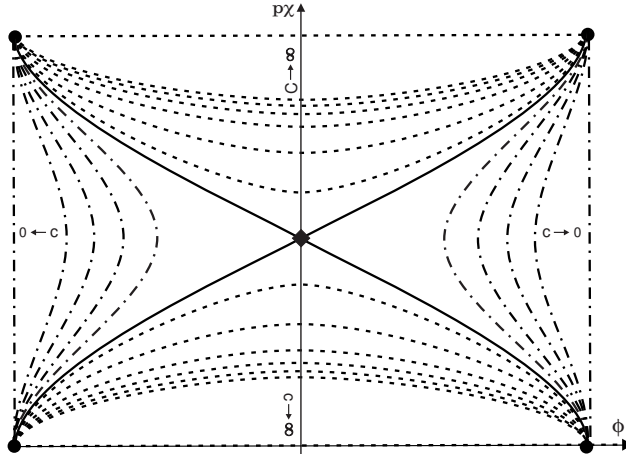


FIG. 5: Orbits from model 1 given for: $0 \leq C < p$ (dash-dotted line), $C = p$ (solid line), and $p < C \leq \infty$ (dashed line).

There are three type of BPS sectors connecting pairs of adjacent minima, namely: vv_1 for $0 \leq C < p$, vw for $C = p$, and vv_2 for $p < C \leq \infty$. The tensions of the BPS states are $t_{vv_1} = t_{vv_2} = 2|\eta|$, and $t_{vw} = |\eta|$. Using the curve (32), the BPS equations (29) and (30) decouple and can be rewritten as, for $C \in (0, \infty)$

$$\frac{d\phi}{dx} = \eta \cos(\phi) [1 - D^{2\nu} \cos^{2\nu}(\phi)]^{\frac{1}{2}} \quad (33)$$

$$\frac{d\chi}{dx} = -\eta p \sin(p\chi) [1 - E^{2/\nu} \sin^{2/\nu}(p\chi)]^{\frac{1}{2}} \quad (34)$$

where $D = 1/Cp$, $E = C^2/p^2$, and $\nu = p^2$. In general, we cannot obtain the analytical solutions of the equations (33) and (34). For this reason, we present some numerical solutions for each kind of orbit, in the following.

Firstly, we investigate the existence of kinks in the vv_1 sector. For simplicity, we consider $C = 0$, which leads to orbits in the form of straight line segments connecting two vertical adjacent v minima, with $\phi = (2k + 1)\pi/2$. This reduces the potential (27) to

$$V = \frac{1}{2} \eta^2 p^2 \sin^2(p\chi) \quad (35)$$

The BPS equations (29) and (30) have the kink and antikink solutions:

$$\begin{aligned} \phi_{vv_1}(x) &= (2k + 1) \frac{\pi}{2} \\ \chi_{vv_1}(x) &= \pm \frac{1}{p} \arccos(\pm \tanh(\eta p^2 x)) + k \frac{\pi}{p} \end{aligned}$$

In Fig. 6, we plot generic numerical solutions for $0 < C < p$.

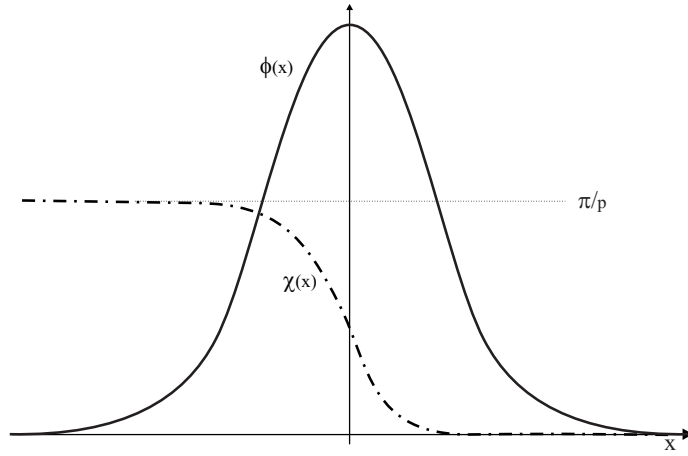
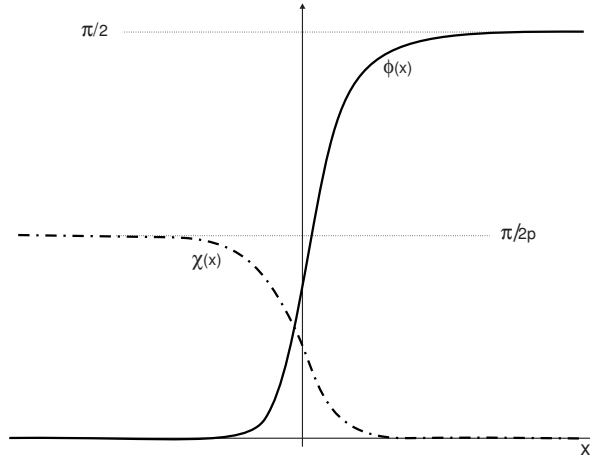
In the vw sector, the numerical solutions for $C = 1/p$ are depicted in Fig. 7.

Finally, we examine the vv_2 sector. Two horizontal adjacent v minima are connected by the straight line orbit $p\chi = k\pi$, for $C = \infty$. In this case, the potential (27) reduces to the form of Eq. (8). Thus, the kink and antikink solutions of the BPS equations are

$$\chi_{vv_2}(x) = k \frac{\pi}{p} \quad (36)$$

$$\phi_{vv_2}(x) = \pm \arcsin(\tanh(\eta x)) + k\pi \quad (37)$$

In Fig. 8, we show numerical solutions in the more general case, for $p < C < \infty$.

FIG. 6: Numerical solutions for vv_1 sector.FIG. 7: Numerical solutions for vw sector.

B. Model 2

Now we explore the second model, described by the potential (27) with $0 < r < 1$. From the superpotential (28) the first-order equations are

$$\frac{d\phi}{dx} = \eta [r + \cos(\phi) \cos(p\chi)] \quad (38)$$

$$\frac{d\chi}{dx} = -\eta p \sin(\phi) \sin(p\chi) \quad (39)$$

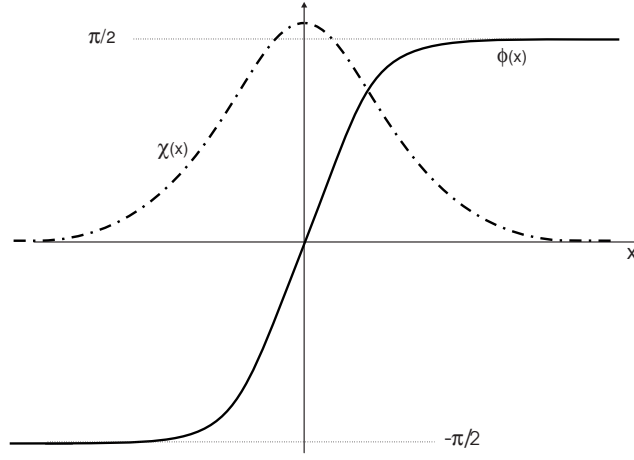
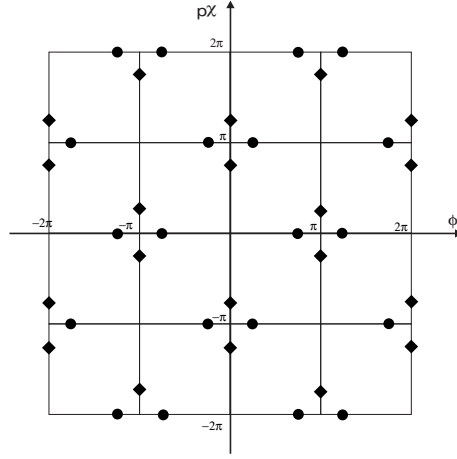
The set of minima are given by $v_{n,m} = (\pm[(1+(-1)^m)\pi/2 - \alpha]/p + 2n\pi, m\pi/p)$ and $w_{n,m} = (n\pi, \pm[(1+(-1)^n)\pi/2 - \alpha]/p + 2m\pi/p)$, with $\alpha = \arccos(r)$. In Fig. 9 we depict the minima in the plane $(\phi, p\chi)$.

To obtain the most general solution to the first-order equations (38) and (39), we integrate the ordinary differential equation

$$\frac{d\phi}{d\chi} = -r \frac{1}{p} \csc(\phi) \csc(p\chi) - \frac{1}{p} \cot(\phi) \cot(p\chi) \quad (40)$$

which admits the integrating factor $\sin^{-\sigma}(p\chi)$, with $\sigma = 1 + 1/p^2$ that determine all the orbits as the family of curves

$$\cos(\phi) = F(\chi) = \frac{1}{p} \sin^{\sigma-1}(p\chi) \left[C + r \int \sin^{-\sigma}(p\chi) d\chi \right] \quad (41)$$

FIG. 8: Numerical solutions for vv_2 sector.FIG. 9: The minima of model 2 potential. The minima v are represented by balls and w by losangles.

where C is a real integration constant. In Fig. 10, we depict behavior of a particular orbit with C , in the family (41), where the critical values are $C_1 \approx -2.734$ and $C_2 \approx 2.734$, for $p = 1/2$ and $r = 1/2$.

There are five different BPS sectors connecting pairs of adjacent minima. They are vv_1 for $-\infty \leq C < C_1$, vw_1 for $C = C_1$, vv_3 for $C_1 < C < C_2$, vw_2 for $C = C_2$, and vv_2 for $C_2 < C \leq \infty$. The tensions of the BPS states are $t_{vv_1} = 2|\eta[\alpha r - \sin(\alpha)]|$, $t_{vv_2} = 2|\eta[(\pi - \alpha)r + \sin(\alpha)]|$, $t_{vv_3} = \frac{1}{2}(t_{vv_1} + t_{vv_2})$, $t_{vw_1} = \frac{1}{2}t_{vv_1}$, and $t_{vw_2} = \frac{1}{2}t_{vv_2}$.

Using the curve (41), the BPS equation (39) decouples, and can be rewritten in the form, for $C \neq \pm\infty$,

$$\frac{d\chi}{dx} = -\eta p \sin(p\chi) [1 - F^2(\chi)]^{\frac{1}{2}} \quad (42)$$

We have been unable to obtain the general solutions of the above equation (42). For this reason, we present some numerical solutions for the several BPS sectors.

Firstly, we investigate the existence of kinks in the vv_1 and vv_2 sectors. Two horizontal adjacent minima are connected by the orbit $p\chi = k\pi$, for $C = -\infty$ and $C = \infty$. In this case, the BPS equations (29) and (30) reduce to

$$\frac{d\phi}{dx} = \eta [r \pm \cos(\phi)] \quad (43)$$

$$\frac{d\chi}{dx} = 0 \quad (44)$$

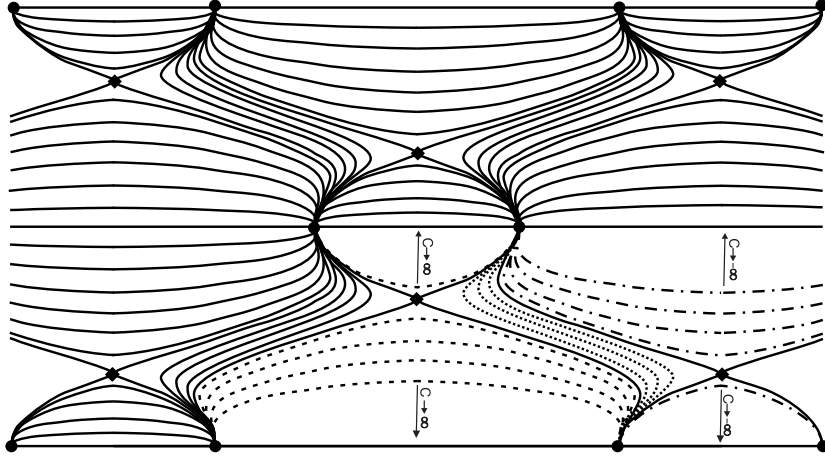


FIG. 10: Orbits given for: $-\infty < C < C_1$ (dash-dotted line), $C = C_1$ (solid line between dash-dotted and dotted lines), $C_1 < C < C_2$ (dotted line), $C = C_2$ (solid line between dotted and dashed lines), $C_2 < C < \infty$ (dashed line).

The potential (27) becomes

$$V_{\pm} = \frac{1}{2}\eta^2 [r \pm \cos(\phi)]^2 \quad (45)$$

These potentials can be obtained from Eq. (10) with $\lambda = \frac{\eta}{2}\sqrt{1-r^2}$, $v = 1/2$, and $\alpha = \sqrt{\frac{1-r}{1+r}}$ or $\sqrt{\frac{1+r}{1-r}}$, for V_+ or V_- , respectively. The solutions are given from Eq. (11) and Eq. (12). For the potential V_+ the kink and antikink solutions are:

$$\chi_{vv_1}(x) = \chi_{vv_2}(x) = 2n\frac{\pi}{p} \quad (46)$$

and

$$\phi_{vv_1}(x) = (2n+1)\pi \pm 2 \arctan\left[\sqrt{\frac{1-r}{1+r}} \tanh\left(\frac{\eta}{2}\sqrt{1-r^2}x\right)\right] \quad (47)$$

and

$$\phi_{vv_2}(x) = 2n\pi \pm 2 \arctan\left[\sqrt{\frac{1+r}{1-r}} \tanh\left(\frac{\eta}{2}\sqrt{1-r^2}x\right)\right] \quad (48)$$

For the potential V_- the procedure is similar. We get

$$\chi_{vv_1}(x) = \chi_{vv_2}(x) = (2n+1)\frac{\pi}{p} \quad (49)$$

and

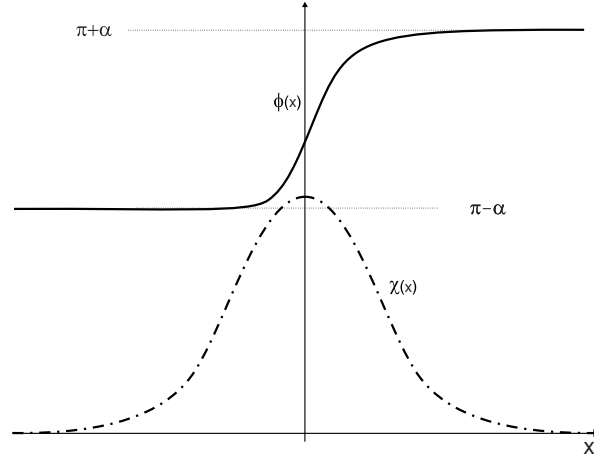
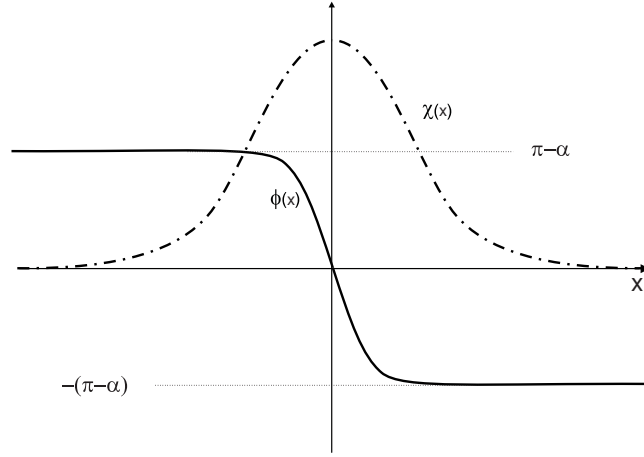
$$\phi_{vv_1}(x) = 2n\pi \pm 2 \arctan\left[\sqrt{\frac{1-r}{1+r}} \tanh\left(\frac{\eta}{2}\sqrt{1-r^2}x\right)\right] \quad (50)$$

and

$$\phi_{vv_2}(x) = (2n+1)\pi \pm 2 \arctan\left[\sqrt{\frac{1+r}{1-r}} \tanh\left(\frac{\eta}{2}\sqrt{1-r^2}x\right)\right] \quad (51)$$

The numerical solutions are presented in figs. 11 and 12, for $-\infty < C < C_1$ and $C_2 < C < \infty$, respectively.

Kinks in the vv_1 , vv_3 and vv_2 sectors are displayed numerically in figs. 13, 14, and 15, for $C = C_1$, $C_1 < C < C_2$, and $C = C_2$, respectively.

FIG. 11: Numerical solutions for vv_1 sector.FIG. 12: Numerical solutions for vv_2 sector.

C. Model 3

The third model is given by the potential (27) with $r \geq 1$. There is a set of minima at the points $u_{n,m} = (2n\pi, (2m+1)\pi/p)$ and $v_{n,m} = ((2n+1)\pi, 2m\pi/p)$. In Fig. 16 we show these minima in the plane $(\phi, p\chi)$.

Here, the first-order equations are (38) and (39). Thus, the orbits are described by (41). There are two kinds of BPS sectors connecting pairs of adjacent minima in this case, namely uu or vv for adjacent horizontal minima, and uv for adjacent diagonal minima. The tensions of the BPS states are $t_{uu} = t_{vv} = |\eta| 2\pi r$ and $t_{uv} = \frac{1}{2} t_{vv}$.

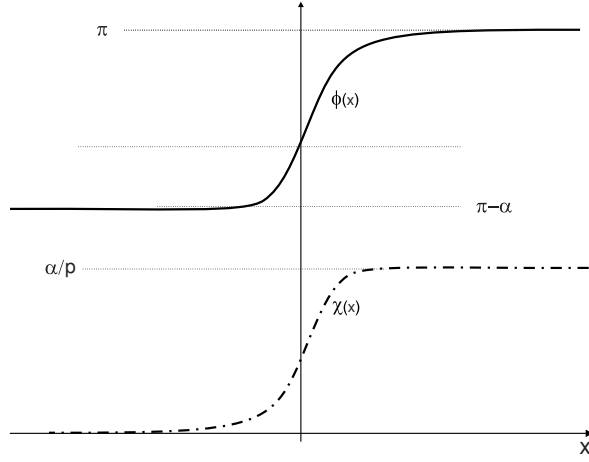
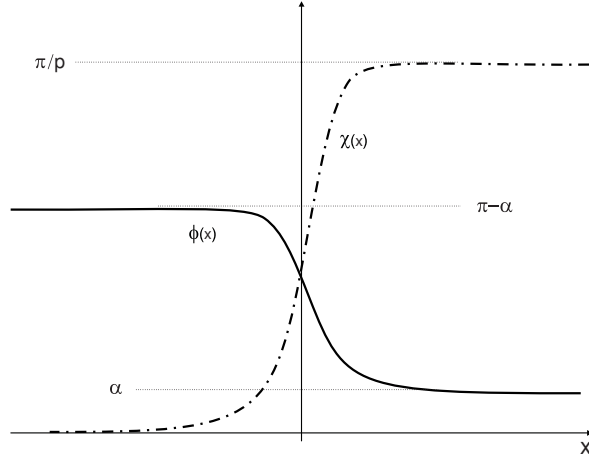
In general, we could not obtain analytical solutions of Eq. (42). For this reason, we present some numerical solutions in the two BPS sectors.

Kinks in the uu or vv sectors are found for $C \rightarrow \infty$, connecting two horizontal adjacent minima, with the orbit as a straight line $p\chi = k\pi$. This reduces the potential (27) to the form (45). In this case, the BPS equations (38) and (39) have the solutions

$$\chi(x) = k \frac{\pi}{p} \quad (52)$$

and

$$\phi(x) = k\pi \pm 2 \arctan \left[\sqrt{\frac{r + (-1)^k}{r - (-1)^k}} \tanh\left(\frac{\eta}{2} \sqrt{r^2 - 1} x\right) \right]. \quad (53)$$

FIG. 13: Numerical solutions for vw_1 sector.FIG. 14: Numerical solutions for vv_3 sector.

Particularly, for $r = 1$ the solutions take the forms:

$$\chi(x) = 2n\frac{\pi}{p}, \quad \phi(x) = \pm 2 \arctan(\eta x) + k\pi \quad (54)$$

or

$$\chi(x) = (2n + 1)\frac{\pi}{p}, \quad \phi(x) = \pm 2 \operatorname{arccot}(\eta x) + k\pi \quad (55)$$

Some numerical solutions in the vu sector, for $C = 10$ and $p = \sqrt{3}/3$, are depicted in Fig. 17.

IV. NON-BPS SOLUTIONS

In this section we search for non-BPS solutions in the models introduced in the former Sec. III. To identify the non-BPS sectors, we investigate the equations of motion corresponding to each one of the three models separately.

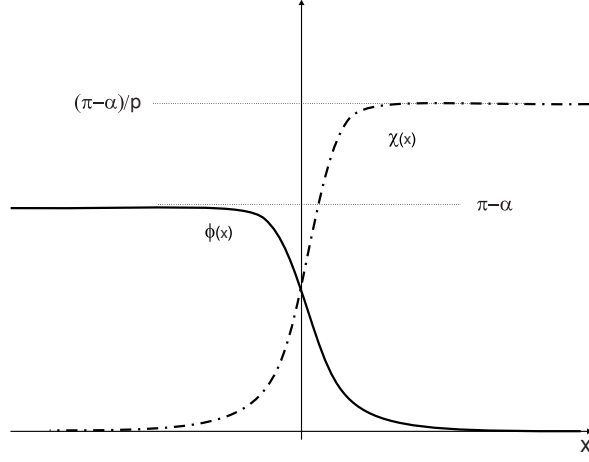
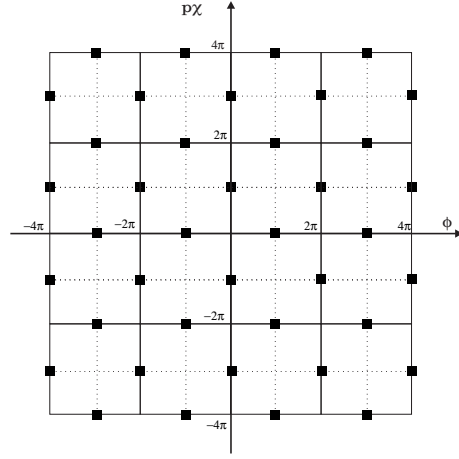
FIG. 15: Numerical solutions for vw_2 sector.

FIG. 16: The set of minima of the model 3.

A. Model 1

From the potential (27), with $r = 0$, we obtain the equations of motion

$$\frac{d^2 \phi}{dx^2} = \frac{1}{2} \eta^2 \sin(2\phi) [p^2 - (1 + p^2) \cos^2(p\chi)] \quad (56)$$

and

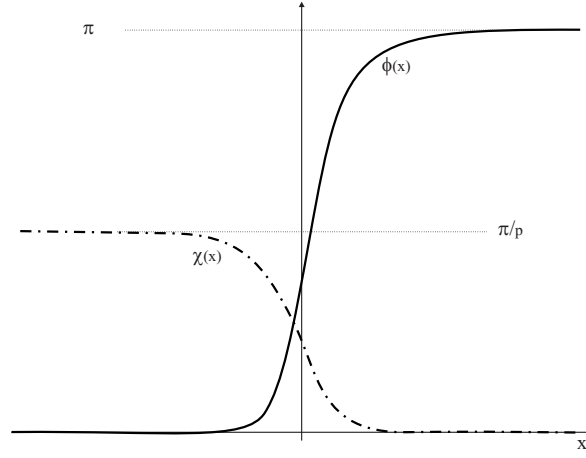
$$\frac{d^2 \chi}{dx^2} = \frac{1}{2} \eta^2 \sin(2p\chi) [p^2 - (1 + p^2) \cos^2(\phi)] \quad (57)$$

There are straight-line orbits connecting two adjacent vertical and horizontal w minima. The vertical orbit reduces the equations of motion (56) and (57) to

$$\frac{d^2 \phi}{dx^2} = 0 \quad (58)$$

and

$$\frac{d^2 \chi}{dx^2} = \frac{1}{2} \eta^2 p^3 \sin^2(2p\chi) \quad (59)$$

FIG. 17: Numerical solutions for uu_2 sector.

The potential (27) reduces to (35), with the kink and antikink solutions

$$\begin{aligned}\phi_{vv_1}(x) &= k\pi \\ \chi_{vv_1}(x) &= \pm \frac{1}{p} \arccos[\pm \tanh(\eta p^2 x)] + k\pi\end{aligned}$$

The horizontal orbit reduces the equations of motion (56) and (57) to

$$\frac{d^2\phi}{dx^2} = \frac{1}{2}\eta^2 p^2 \sin(2\phi) \quad (60)$$

$$\frac{d^2\chi}{dx^2} = 0 \quad (61)$$

The potential (27) becomes $V = \frac{1}{2}\eta^2 p^2 \sin^2(\phi)$, with the kink and antikink solutions

$$\chi_{vv_2}(x) = (2k+1) \frac{\pi}{2p} \quad (62)$$

$$\phi_{vv_2}(x) = \pm \arccos[\pm \tanh(\eta qx)] + k\pi \quad (63)$$

It is interesting to notice that if one considers the plane rotator model to describe the open states in the molecule of deoxyribonucleic acid (DNA), in Ref. [59] the author has obtained the coupled sine-Gordon equations

$$(1 - D^2/C_0^2) \frac{d^2 u}{d\xi^2} = \frac{1}{l^2} \sin(u) + \frac{2}{d^2} \sin\left(\frac{1}{2}u\right) \cos\left(\frac{1}{2}v\right)$$

$$(1 - D^2/C_0^2) \frac{d^2 v}{d\xi^2} = \frac{Q}{l^2} \sin(v) + \frac{2}{d^2} \sin\left(\frac{1}{2}v\right) \cos\left(\frac{1}{2}u\right)$$

with $u = \varphi + \varphi'$ and $v = \varphi - \varphi'$, where D , C_0 , l , Q and d are physical constants, and φ and φ' describe the angular displacements of two plane base-rotators. On the other hand, the equations of motions (56) and (57) can be rewritten in the form

$$\frac{d^2\phi}{dx^2} = \frac{1}{2}\eta^2 \left[\frac{1}{2}(1-p^2) \sin(2\phi) - \frac{1}{2}(1+p^2) \sin(2\phi) \cos(2p\chi) \right] \quad (64)$$

$$\frac{d^2\chi}{dx^2} = \frac{1}{2}\eta^2 \left[\frac{1}{2}(1-p^2) \sin(2p\chi) - \frac{1}{2}(1+p^2) \sin(2p\chi) \cos(2\phi) \right] \quad (65)$$

We notice that this model can be used as an alternative to the DNA model; this will be further examined in another work.

B. Model 2

From the potential (27), with $0 < r < 1$, we obtain the equations of motion

$$\frac{d^2\phi}{dx^2} = \frac{1}{2}\eta^2 \sin(\phi) [p^2 \cos(\phi) \sin^2(p\chi) - p^2 \cos(q\chi) [r + \cos(p\phi) \cos(q\chi)]] \quad (66)$$

$$\frac{d^2\chi}{dx^2} = \frac{1}{2}\eta^2 p \sin(p\chi) [p^2 \cos(p\chi) \sin^2(\phi) - \cos(\phi) [r + \cos(\phi) \cos(p\chi)]] \quad (67)$$

There are straight-line orbits, $\phi = k\pi$, connecting two adjacent vertical w minima. The orbit reduces the potential (27) to $V_{\pm} = \frac{1}{2}\eta^2 [r \pm \cos(p\chi)]^2$. For the potential V_+ , the solutions are

$$\phi_{ww(1,2)}(x) = k\pi, \quad \chi_{ww(1,2)}(x) = \frac{1}{p} \phi_{vv(1,2)}(x) \quad (68)$$

where $\phi_{vv(1,2)}$ are given by (47) and (48), respectively. For the potential V_- , the solutions are

$$\phi_{ww(1,2)}(x) = (2k+1)\pi, \quad \chi_{ww(1,2)}(x) = \frac{1}{p} \phi_{vv(1,2)}(x) \quad (69)$$

where $\phi_{vv(1,2)}$ are given by (50) and (51), respectively.

C. Model 3

From the potential (27), with $r \geq 1$, we obtain the equations of motion (66) and (67). There are straight-line orbits, $\phi = k\pi$, connecting two adjacent vertical u or v minima. The orbit reduces the potential (27) to

$$V = \frac{1}{2}\eta^2 [r + (-1)^k \cos(p\chi)]^2. \quad (70)$$

The solutions are

$$\phi(x) = k\pi, \quad \chi(x) = \frac{1}{p} \tilde{\phi}(x), \quad (71)$$

where $\tilde{\phi}$ is given by eq. (53).

The non-BPS solutions may be unstable, and may decay into stable BPS solutions. The decay of non-BPS states is out of the scope of this work, but it can be done following for instance the lines of Ref. [70].

V. COMMENTS AND CONCLUSIONS

In the present work we have investigated several models described by one and by two real scalar fields. The main investigations concern the search for BPS states, that is, for topological solutions that solve first order differential equations. These solutions minimize the energy to the Bogomol'nyi bound, which is given solely in terms of the superpotential, and the asymptotic value of the corresponding field configurations.

The search for topological solutions is done at the classical level, and we have payed special attention to models introduced in Sec. II, some of them further explored in Sec. III. These investigations have shown how to write the double sine-Gordon model in terms of a superpotential, and to deal with the large and small kinks as BPS states, as solutions to first order differential equations. We have also investigated another model, described by two real scalar fields, defined by the potential of Eq. (27). It is similar to the model first investigated in Ref. [60], although here we deal only with periodic interactions.

The classical investigations that we have developed are of interest in applications to nonlinear science, as for instance in the line of the work presented in Refs. [37, 38, 39, 40], where one uses field theory models to mimic nonlinear interactions in polymeric chains. For instance, the model 1 may be used as an alternative to the ϕ^4 model that is standardly considered to mimic the polyacetylene (PA) chain, where Peierls instability appears due to single and double bond alternation in carbon atoms along the chain. The standard scenario leads to the very nice picture in which the distance carbon-carbon is mapped to the ϕ^4 model with spontaneous symmetry breaking. The need for

spontaneous symmetry breaking is to reproduce the two degenerate states, which describe single-double and double-single bond alternations in the trans or zig-zag PA chain. Of course, this picture can become more interesting if one adds fermions to the system, via the standard Yukawa coupling. The alternative that we propose is to mimic the PA chain with model 1, which is very much similar to the ϕ^4 model at the classical level. We hope to explore this and similar ideas in the near future.

A direct motivation that follows from the present investigations concerns the inclusion of fermions, to see how the fermions change the scenario we have just obtained. Another motivation concerns generalization of the field theory models to the case of complex fields, which may give rise to models engendering the continuum $U(1)$ symmetry. In this new scenario the models admit the presence of vortices, global and local, depending on the gauging of the global symmetry that appears when one changes the real field to a complex one. Furthermore, the two-field model investigated in Sec. III is of direct use to describe interactions between two BEC's, and the corresponding vector solution describes the interface between the interacting condensates, as a good alternative to the recently proposed model of Ref. [67], because in our model the center of the interface is asymmetric, containing different quantities of each one of the two condensates that form the interface. This is more realist than the case studied in [67], where the center of the interface contains equal portions of each one of the two condensates. All the models here introduced are also of interest to pattern formation in spatially extended, periodically forced systems, governed by the Ginzburg-Landau equation. This is a new route, different from the one proposed in [37], and further investigated in [38, 39, 40], which deals with solitons in ferroelectric crystals, in polyethylene, and in Langmuir films. The Ginzburg-Landau equation is appropriate for investigating fronts and interfaces, and their contributions to pattern formation. These and other specific issues are presently under investigation, and we hope to report on them in the near future.

Acknowledgments

The authors would like to thank PROCAD/CAPES and PRONEX/FAPESQ/CNPq for financial support. DB thanks CNPq for partial support, and RM thanks CAPES for a fellowship.

-
- [1] A.H. Eschenfelder, *Magnetic Bubble Technology* (Springer, Berlin, 1981).
 - [2] D. Walgraef, *Spatio-Temporal Pattern Formation* (Springer, New York, 1997).
 - [3] R. Rajaraman, *Solitons and Instantons* (North-Holland, Amsterdam, 1982).
 - [4] A. Vilenkin and E.P.S. Shellard, *Cosmic Strings and Other Topological Defects* (Cambridge, Cambridge, UK, 1994).
 - [5] Y. Kuramoto, *Chemical Oscillations, Waves, and Turbulence* (Springer, Berlin, 1984).
 - [6] B.A. Strukov and A.P. Levanyuk, *Ferroelectric Phenomena in Crystals* (Springer, Berlin, 1998).
 - [7] E.W. Kolb and M.S. Turner, *The Early Universe* (Addison-Wesley, Redwood, CA, 1990).
 - [8] K. Maki and P. Kumar, Phys. Rev. B **14**, 118 (1976); **14**, 3920 (1976).
 - [9] H. Dvey-Aharon, T.J. Sluckin, and P.L. Taylor, Phys. Rev. B **21**, 3700 (1980).
 - [10] C.A. Condat, R.A. Guyer, and M.D. Miller, Phys. Rev. B **27**, 474 (1983).
 - [11] D.K. Campbell, M. Peyrard, P. Sodano, Physica D **19**, 165 (1986).
 - [12] G. Delfino and G. Mussardo, Nucl. Phys. B **516**, 675 (1998).
 - [13] G. Mussardo, V. Riva, and G. Sotkov, Nucl. Phys. B **687**, 189 (2004).
 - [14] R. MacKenzie, Nucl. Phys. B **303**, 149 (1998).
 - [15] J.R. Morris, Phys. Rev. D **52**, 1096 (1995).
 - [16] D. Bazeia, R.F. Ribeiro, and M.M. Santos, Phys. Rev. D **54**, 1852 (1996).
 - [17] F.A. Brito and D. Bazeia, Phys. Rev. D **56**, 7869 (1997).
 - [18] J.D. Edelstein, M.L. Trobo, F.A. Brito, and D. Bazeia, Phys. Rev. D **57**, 7561 (1998).
 - [19] J.R. Morris, Int. J. Mod. Phys. A **13**, 1115 (1998).
 - [20] D. Bazeia, H. Boschi-Filho, and F.A. Brito, J. High Energy Phys. **04**, 028 (1999).
 - [21] G.W. Gibbons and P.K. Townsend, Phys. Rev. Lett. **83**, 1727 (1999).
 - [22] P.M. Saffin, Phys. Rev. Lett. **83**, 4249 (1999).
 - [23] H. Oda, K. Naganuma, and N. Sakai, Phys. Lett. B **471**, 148 (1999).
 - [24] D. Bazeia and F.A. Brito, Phys. Rev. Lett. **84**, 1094 (2000).
 - [25] D. Bazeia and F.A. Brito, Phys. Rev. D **61**, 105019 (2000).
 - [26] M. Shifman and T. ter Veldhuis, Phys. Rev. D **62**, 065004 (2000).
 - [27] A. Alonso Izquierdo, M.A. Gonzalez Leon, and J. Mateos Guilarte Phys. Lett. B **480**, 373 (2000).
 - [28] R. Hofmann, Phys. Rev. D **62**, 065012 (2000).
 - [29] D. Bazeia and F.A. Brito, Phys. Rev. D **62**, 101701(R) (2000).
 - [30] D. Binosi and T. ter Veldhuis, Phys. Rev. D **63**, 085016 (2001).
 - [31] F.A. Brito and D. Bazeia, Phys. Rev. D **64**, 065022 (2001).

- [32] M. Naganuma and M. Nitta, *Prog. Theor. Phys.* **105**, 501 (2001).
- [33] M. Naganuma, M. Nitta, and N. Sakai, *Phys. Rev. D* **65**, 045016 (2002).
- [34] J.H. Schwartz, *Nucl. Phys. B (Proc. Suppl.)* **55**, 1 (1997).
- [35] J. Maldacena, *Adv. Theor. Math. Phys.* **2**, 231 (1998).
- [36] A. Giveon and D. Kutasov, *Rev. Mod. Phys.* **71**, 983 (1999).
- [37] D. Bazeia, R.F. Ribeiro, and M.M. Santos, *Phys. Rev. E* **54**, 2943 (1996).
- [38] D. Bazeia and E. Ventura, *Chem. Phys. Lett.* **303**, 341 (1999).
- [39] E. Ventura, A.M. Simas, and D. Bazeia, *Chem. Phys. Lett.* **320**, 587 (2000).
- [40] D. Bazeia, V.B.P. Leite, B.H.B. Lima, and F. Moraes, *Chem. Phys. Lett.* **340**, 205 (2001).
- [41] B. Denardo *et al.*, *Phys. Rev. Lett.* **68**, 1730 (1992).
- [42] M. Torres, J.P. Adrados, and F.R. Montero de Espinosa, *Nature*, **398**, 114 (1998).
- [43] P. Coulet, J. Lega, B. Houchmanzadeh, and J. Lajzerowicz, *Phys. Rev. Lett.* **65**, 1352 (1990).
- [44] P. Collet and J.-P. Eckmann, *Instabilities and Fronts in Extended Systems* (Princeton, Princeton/NJ, 1990).
- [45] C. Elphick, A. Hagberg, and E. Meron, *Phys. Rev. Lett.* **80**, 5007 (1998); *Phys. Rev. E* **59**, 5285 (1999).
- [46] G. Bertotti, *Hysteresis in Magnetism* (Academic, San Diego/CA, 1998).
- [47] E.B. Bogomol'nyi, *Sov. J. Nucl. Phys.* **24**, 449 (1976).
- [48] M.K. Prasad and C.M. Sommerfield, *Phys. Rev. Lett.* **35**, 760 (1975).
- [49] D. Bazeia, J. Menezes, and M.M. Santos, *Phys. Lett. B* **521**, 418 (2001).
- [50] D. Bazeia, J. Menezes, and M.M. Santos, *Nucl. Phys. B* **636**, 132 (2002).
- [51] D. Bazeia, L. Losano, and J.M.C. Malbouisson, *Phys. Rev. D* **66**, 101701(R) (2002).
- [52] C.A. Almeida, D. Bazeia, L. Losano, and J.M.C. Malbouisson, *Phys. Rev. D* **69**, 06 (2004).
- [53] A.N. Bogdanov, U.K. Rossler, M. Wolf, and K.-H. Müller, *Phys. Rev. B* **66**, 214410 (2002).
- [54] C.A.G. Almeida, D. Bazeia, and L. Losano, *J. Phys. A* **34**, 3351 (2001).
- [55] Y.S. Kivshar, D.E. Pelinovsky, T. Cretegny, and M. Peyrard, *Phys. Rev. Lett.* **80**, 5032 (1998).
- [56] A. Alonso Izquierdo, M.A. Gonzalez Leon, and J. Mateos Guilarte, *Phys. Rev. D* **65**, 085012 (2002).
- [57] D. Bazeia, W. Freire, L. Losano, and R.F. Ribeiro, *Mod. Phys. Lett. A* **17**, 1945 (2002).
- [58] J. Pouget and G.A. Maugin, *Phys. Rev. B* **30**, 5306 (1984).
- [59] C.T. Zhang, *Phys. Rev. A* **35**, 886 (1987); **40**, 2148 (1989).
- [60] D. Bazeia, M.J. dos Santos, and R.F. Ribeiro, *Phys. Lett. A* **208**, 84 (1995).
- [61] B. Horowitz, J.A. Krumhansl, and E. Domany, *Phys. Rev. Lett.* **14**, 778 (1977).
- [62] S.E. Trullinger and R.M. DeLeonardis, *Phys. Rev. A* **20**, 2225 (1979).
- [63] S. Theodorakis, *Phys. Rev. D* **60**, 125004 (1999).
- [64] M.A. Shifman and M.B. Voloshin, *Phys. Rev. D* **57**, 2590 (1998).
- [65] C.J. Myatt *et al.*, *Phys. Rev. Lett.* **78**, 586 (1997).
- [66] E. Timmermans, *Phys. Rev. Lett.* **81**, 5718 (1998).
- [67] S. Coen and M. Haelterman, *Phys. Rev. Lett.* **87**, 140401 (2001).
- [68] D. Bazeia, *Phys. Rev. D* **60**, 067705 (1999).
- [69] M.A. Lohe, *Phys. Rev. D* **20**, 3120 (1979).
- [70] N. Riazi, A. Azizi, and S.M. Zebarjad, *Phys. Rev. D* **66**, 065003 (2002).